The structure shown in Fig. 3 is the same as that studied in [5]. Following the same transformations and assumptions used in [5], the final formulas for the capacitances of the equivalent π-network of the CCPW gap are given by

$$C_p = 4\varepsilon_0\varepsilon_{eff}\left[\frac{K(k_3)}{K(k_3')}K(k)\frac{S}{2} - \frac{K(k)}{K(k')}L\right]$$

$$C_s = 2\varepsilon_0\varepsilon_{eff}\left[\frac{K(k_2)}{K(k_2')} - \frac{K(k_3)}{K(k_3')}\right]K(k)\frac{S}{2}$$

where

$$k = \frac{v_1 + \alpha v_0^2}{v_0(1 + \alpha v_1)}$$

$$v_0 = \frac{\phi_0}{\sqrt{\pi^2 - \phi_0^2}} \quad v_1 = \frac{\phi_1}{\sqrt{\pi^2 - \phi_1^2}}$$

$$\frac{K(k_1)}{K(k_1')} = \frac{L + G/2}{(S/2)\cdot K(k')}$$

$$k_2 = sn\left[\frac{L}{L + G/2}K(k_1), k_1\right]$$

$$k_3 = k_1 \cdot k_2$$

$$\varepsilon_{eff} = \frac{1 + \varepsilon_r}{2}$$

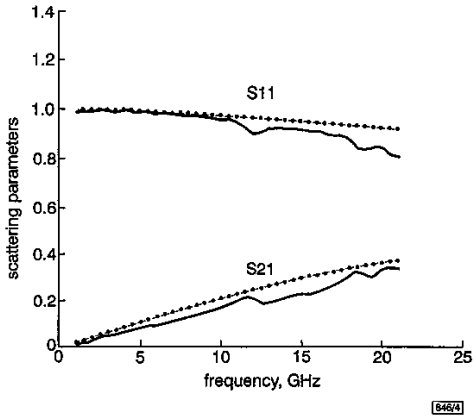

Fig. 4 *Scattering parameters against frequency for structure: b = 7mm, S = 2mm, $W_1 = W_2 = 0.4$mm, G = 1.2mm, $\varepsilon_r = 2.01$*

---- CMM
——— FDTD

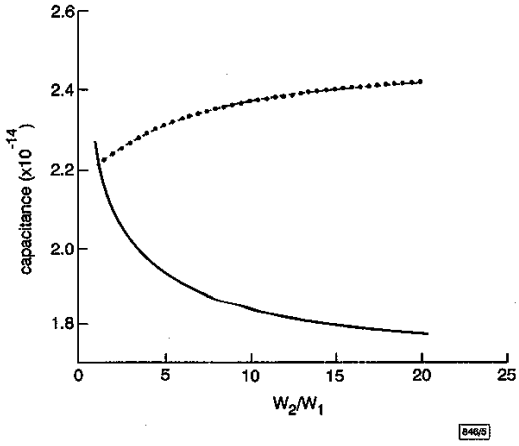

Fig. 5 *Effect of slot asymmetry on capacitances C_p and C_s for structure: b = 7mm, S = 2mm, $W_1 = W_2 = 0.4$mm, G = 1.2mm, $\varepsilon_r = 2.01$*

---- *Cs*
——— *C_p*

Numerical results: The previous formulas are used to evaluate the capacitances of the equivalent π-network, from which the scattering parameters of the gap are computed. Fig. 4 shows the CMM results, compared to those obtained using the FDTD technique. The agreement is very good in the whole frequency range (0–20GHz), which shows that quasi-TEM approximation for the studied CCPW is valid up to 20GHz. It is observed that the difference between the two methods is larger around 11.5GHz and 18.5GHz. These two frequencies were identified to be the cutoff frequencies of the TM_{01} and TM_{11} modes that are excited in a circular waveguide completely filled with $\varepsilon_r = 2.0$ dielectric material. This could be caused by the longitudinal electric field component that exists in the gap between the two centre conductors. It is interesting to note that the dominant TE_{11} mode, which has a cutoff frequency of 9GHz, does not affect the gap response. Fig. 5 shows the effect of slot asymmetry on the capacitances C_s and C_p. It can be seen that as W_1/W_2 increases, C_s increases and C_p decreases. It is also observed that the change in C_s is small, but the change in C_p is large. Moreover, it has been found that the curvature effect on the capacitances is negligible as long as the circumference of the CCPW is ten times $(S + W_1 + W_2)$.

Conclusions: Closed-form expressions for the capacitances of the equivalent π-network of a CCPW gap with asymmetric slot widths have been derived using the conformal mapping technique. This method has been validated by comparing the results with those obtained using the FDTD technique. The effect of various parameters on the characteristics of the CCPW gap has been studied.

17 August 1999
Electronics Letters Online No: 19991283
DOI: 10.1049/el:19991283

A. Al-Zoubi and N. Dib (*Department of Electrical Engineering, Jordan University of Science and Technology, PO Box 3030, Irbid, Jordan*)

E-mail: nihad@just.edu.jo

References

1 SU, H.C., and WONG, K.L.: 'Dispersion characteristics of cylindrical coplanar waveguide', *IEEE Trans. Microw. Theory Tech.*, 1996, **44**, (11), pp. 2120–2122

2 DIB, N., WELLER, T., SCARDELLETTI, M., and IMPARATO, M.: 'Analysis of cylindrical transmission lines with the finite difference time domain method', *IEEE Trans. Microw. Theory Tech.*, 1999, pp. 509–512

3 DIB, N., and AL-ZOUBI, A.: 'Quasi-static analysis of asymmetrical cylindrical coplanar waveguide with finite-extent ground', *Int.* to be published in *J. Electron.*

4 DIB, N., WELLER, T., and SCARDELLETTI, M.: 'Analysis of 3-D cylindrical structures using the finite difference time domain method'. 1998 Int. Microw. Symp. Dig., pp. 925–928

5 GEVORGIAN, S., DELENIV, A., MARTINSSON, T., GAL'CHENKO, S., LINNER, P., and VENDIK, I.: 'CAD model of a gap in a coplanar waveguide', *Int. J. Microw. Millim.-Wave Comput.-Aided Eng.*, 1996, **6**, (5), pp. 369–377

Optimum line length between microwave circuit modules for flattest transfer characteristic

Jong-Sik Lim and Sangwook Nam

A method is presented for determining the optimum length of the connecting line between microwave circuit modules that enables the flattest transfer characteristic to be obtained. Sensitivity analysis has been performed to verify that a small change in the phase of the S_{11} and S_{22} parameters of the connected modules is desirable for obtaining a flat transfer characteristic.

Introduction: In the design of multistage microwave circuits such as amplifiers using single-stage circuit modules, the transferred signal and its flatness fluctuates depending on the length of the connecting line between the modules. This is caused by the fact that the module is not perfectly matched, i.e. the S_{11} and S_{22} of the modules are not equal to zero [1 – 4]. Fig. 1 shows a two-stage amplifier composed of two identical single-stage modules. The

connecting line length between the modules is designated as l. Fig. 1 shows a 50Ω line with length $l/2$ attached to the end of each matching network of the single-stage module. The total gain and flatness of this two-stage amplifier depend on the connecting length, as shown in Fig. 4. The optimum length must therefore be found in order to obtain the flattest transfer characteristic. However, the connecting length of the 50Ω line is usually determined arbitrarily without detailed consideration of the effect of the arbitrary length between the modules. In this Letter, a method for determining the optimum connecting length between the modules is presented that enables the flattest transfer characteristic to be obtained.

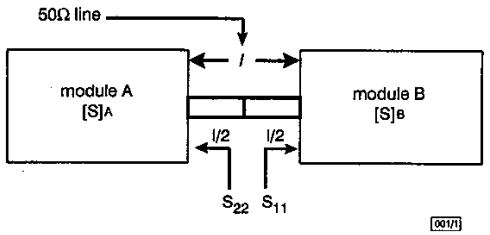

Fig. 1 *Connecting line between circuit modules*

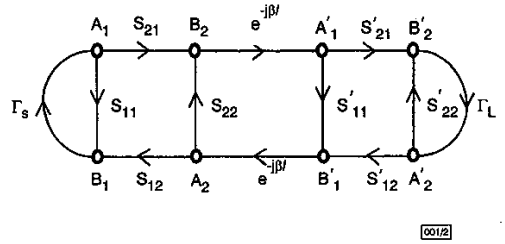

Fig. 2 *Signal flow graph for the connection of two circuit modules*

Analysis of signal transfer between modules: An analysis of the signal transfer using the signal flow graph [4] shown in Fig. 2 gives the transfer function T for the connection section given in eqn. 1. The transfer characteristic fluctuates as the length l changes. Eqn. 2, derived from eqn. 1 with Γ_S and Γ_L matched or connected to the 50Ω port, represents the connecting length for obtaining the maximum transfer at each frequency.

$$T = \frac{S_{21}S'_{21}e^{-j\beta\ell}}{1 - S_{22}S'_{11}e^{-j2\beta\ell}} \tag{1}$$

$$\ell = \frac{1}{4\pi}\tan^{-1}\left(\frac{a_1b_2 + a_2b_1}{a_1a_2 - b_1b_2}\right)[\lambda] \tag{2}$$

where $S'_{11} = a_1 + jb_1$, $S_{22} = a_2 + jb_2$.

Fig. 3 shows the performance of a single-stage amplifier module, which consists of an active device, and matching input and output networks with $l/2 = 0$. When the two identical modules are connected, $[S]_A = [S]_B$ and the total gain fluctuates for various l as predicted by eqn. 1.

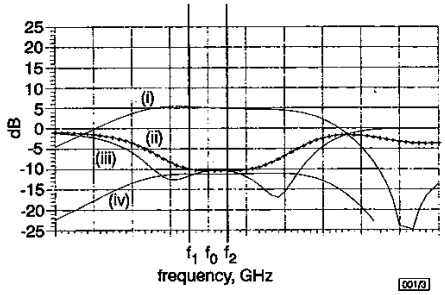

Fig. 3 *S-parameters of single-stage amplifier module*

(i) S_{21}
(ii) S_{11}
(iii) S_{22}
(iv) S_{12}

Fig. 4 shows the gain curves of an amplifier composed of two single-stage amplifier modules at several frequencies for a connecting length of 0 – 0.5λ. The usefulness of eqn. 2 can be seen in Fig. 4. The connecting length for obtaining the maximum gain at each frequency shown in Fig. 4 agrees exactly with the value in eqn. 2. Fig. 4 also presents some important information. First, the variation of gain and flatness of the total amplifier for different connecting lengths is shown. Secondly, the lengths for obtaining maximum transfer at each frequency are shown. The optimum length and condition for obtaining the flattest transfer characteristic can be derived from Fig. 4.

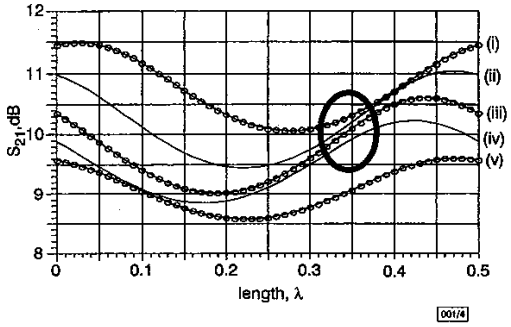

Fig. 4 *Gain curves of two-stage amplifier for connecting lengths of 0 – 0.5λ at different frequencies*

(i) f_1
(ii) f_1
(iii) f_o
(iv) f_2
(v) f_2

Conditions for obtaining flattest transfer characteristic: Let f_o be the centre frequency when the bandwidth is $f_2 - f_1$ and $f_2 > f_1$. In general, l will be determined at f_o. This may cause serious problems at other frequencies. Although the realised connection length is physically fixed and constant at f_o, the length in lambda units (electrical length) varies at each frequency, i.e. the length $l_o[\lambda_o]$ at f_o is no longer $l_o[\lambda_1]$ at f_1 and $l_o[\lambda_2]$ at f_2. $l_o[\lambda_o]$ at f_o should be converted to $l_1[\lambda_1]$ and $l_2[\lambda_2]$ at f_1 and f_2, respectively, as described in eqn. 3. Here λ_i denotes the wavelength at f_i, and $i = 1, 2$.

$$\ell_1 = \ell_o\frac{f_1}{f_o}[\lambda_1] \quad \text{and} \quad \ell_2 = \ell_o\frac{f_2}{f_o}[\lambda_2] \tag{3}$$

$$\Delta\ell_{1o} = \Delta\ell_{o2} = \ell_o[\lambda_o] - \ell_1[\lambda_1] = \ell_2[\lambda_2] - \ell_o[\lambda_o] \tag{4}$$

$$\ell_o[\lambda_o] = \frac{\ell_1[\lambda_1] + \ell_2[\lambda_2]}{2} \tag{5}$$

Since the relations $l_1[\lambda_1] < l_o[\lambda_o] < l_2[\lambda_2]$ always hold, Δl_{1o} and Δl_{o2} can be defined as in eqn. 4. This seems simple but has great significance. If an amplifier composed of two single-stage modules has the flattest gain characteristic, then the gain curves shown in Fig. 4 should describe a region similar in shape to that in Fig. 5, i.e. for a fixed(flat) gain G_f, the position of the S_{21} curve at f_1 should be located to the left of that at f_o, and the S_{21} curve at f_2 should be located to the right of f_o. Eqn. 5 should also be satisfied.

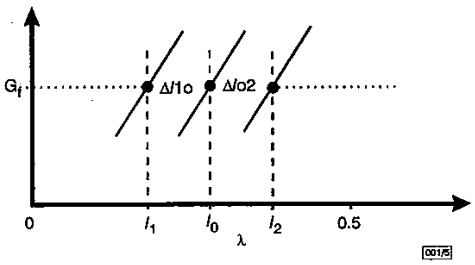

Fig. 5 *Condition for obtaining flattest gain with two-stage amplifier*

S_{21} curves:
(i) f_1
(ii) f_o
(iii) f_2

Fig. 5 shows the ideal condition for obtaining the flattest gain characteristic, i.e. when the S_{21} curve at f_o crosses the point (l_o, G_f), the S_{21} curve crosses (l_1, G_f) at f_1 and (l_2, G_f) at f_2. At this point, eqn. 5 is satisfied exactly and the gain is G_f at f_1, f_2 and f_o. In Fig. 4, $l = 0.33 - 0.34\lambda$ at f_o presents the most desirable condition for obtaining flat gain. The overall performance of a two-stage amplifier is optimum at this length, as shown in Fig. 6.

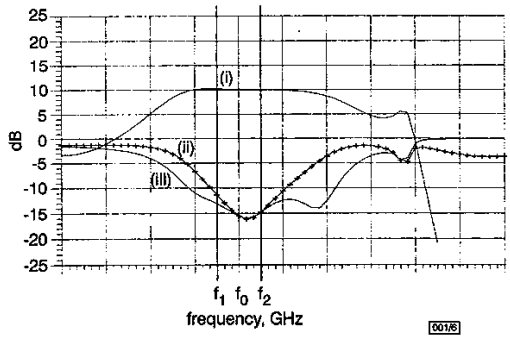

Fig. 6 *Gain flatness of two-stage amplifier with $l = 0.34\lambda$ at f_o*

(i) S_{21}
(ii) S_{11}
(iii) S_{22}

Sensitivity analysis of connecting length: The relations between the connecting length and S'_{11} and S_{22} of the module can be analysed by means of a sensitivity analysis for l. The connecting length is a function of a_1, b_1, a_2, b_2, i.e. S'_{11} and S_{22}, as shown in eqn. 2. To determine the effects of a_1, b_1, a_2, b_2 when calculating the change in l at the next frequency(Δl), sensitivity factors are introduced as shown in eqn. 6. After mathematical manipulations, we can describe Δl, the change in l from one frequency to another, as shown in eqn. 7:

$$S_{a_1} = \frac{\Delta \ell}{\Delta a_1} \quad S_{b_1} = \frac{\Delta \ell}{\Delta b_1} \quad S_{a_2} = \frac{\Delta \ell}{\Delta a_2} \quad S_{b_2} = \frac{\Delta \ell}{\Delta b_2} \quad (6)$$

$$\Delta \ell = \frac{1}{4\pi}\left(\frac{-b_1\Delta a_1 + a_1\Delta b_1}{M_{11}^2} + \frac{-b_2\Delta a_2 + a_2\Delta b_2}{M_{22}^2}\right) \quad (7)$$

where $M_{11}^2 = a_1^2 + b_1^2$ and $M_{22}^2 = a_2^2 + b_2^2$. According to eqn. 7, the main factors which determine Δl are not only a_1, b_1, a_2, b_2, but Δa_1, Δb_1, Δa_2 and Δb_2. This shows that the phases of S'_{11} and S_{22} of the connected module play an important role in determinating Δl. Fig. 4 will show a similar region to that in Fig. 5 if there are small changes in the phases of S_{11} and S_{22} of the module, i.e. if there is a small variation in Δa_1, Δb_1, Δa_2 and Δb_2.

Conclusions: We have developed a method for determining the the optimum connecting length between microwave circuit modules that enables the flattest transfer characteristic to be obtained. The total gain shape fluctuates at various connecting lengths because the module is not perfectly matched and the length l_o at f_o is not same at other frequencies. It has been proven by means of a sensitivity analysis that the optimum length for obtaining a flat transfer characteristic and the condition that dictates whether flat transfer is obtainable are dependent on the change in phases of S'_{11} and S_{22} of the connected module.

The technique in this Letter can be applied to the design of microwave and millimetre-wave multistage amplifiers, MCMs (multi chip modules), multi-circuit integrated MMIC-like transceivers, and other kinds of circuit with HMIC or MMIC modules.

24 August 1999
Electronics Letters Online No: 19991284
DOI: 10.1049/el:19991284

Jong-Sik Lim and Sangwook Nam (*School of Electrical Engineering, Seoul National University, San 56-1, Shilim-Dong, Kwanak-Gu, Seoul, 151-742, Republic of Korea*)

References

1 MELLOR, D.J., and LINVILL, J.G.: 'Synthesis of interstage networks of prescribed gain versus frequency slopes', *IEEE Trans. Microwave Theory Tech.*, 1975, **MTT-23**, pp. 1013–1020
2 VILLAR, J.C., and PEREZ, F.: 'Graphic design of matching and interstage lossy networks for microwave transistor amplifier', *IEEE Trans. Microwave Theory Tech.*, 1985, **MTT-33**, pp. 210–215
3 MACCHIARELLA, G., RAGGI, A., and LORENZO, E.D.: 'Design criteria for multistage microwave amplifiers with match requirements at input and output', *IEEE Trans. Microwave Theory Tech.*, 1993, **MTT-41**, pp. 1294–1298
4 GONZALEZ, G.: 'Microwave transistor amplifier analysis and design' (Prentice-Hall, New Jersey, 1984)

320Gbit/s (32 × 10.7Gbit/s) error-free transmission over 7280km using dispersion flattened fibre link with standard SMF and slope compensating DCF

K. Tanaka, T. Tsuritani, N. Edagawa and M. Suzuki

320Gbit/s (32 × 10.7Gbit/s) error-free transmission over 7280km has been successfully achieved with an average Q-factor of 15.9dB in dispersion flattened systems using standard singlemode fibre and slope compensating dispersion compensation fibre.

Introduction: The recent development of WDM technology has led to a remarkable capacity increase in long-haul optical fibre communication systems [1 – 4]. For further progress, broadband amplifiers and a dispersion flattened fibre link are required, since the bit error performance after long distance transmission is degraded by the interaction between nonlinearity and large accumulated dispersion due to the dispersion slope for the channels far from the zero-dispersion wavelength [1]. To overcome this problem, various dispersion slope compensation schemes have been reported [5 – 8]. In particular, the method of constructing dispersion flattened transmission spans with standard singlemode fibre (SMF) and slope compensating dispersion compensation fibre (SCDCF) [5 – 7] is quite attractive, because the high dispersion and large effective area of SMF enable a reduction in nonlinear effects such as four-wave mixing (FWM) and cross-phase modulation (XPM) to be obtained.

In this Letter, we report successful 320Gbit/s (32 × 10.7Gbit/s) WDM transmission over 7280km using dispersion flattened transmission spans combined with SMF and SCDCF.

Experiment: Fig. 1 shows a schematic diagram of the experimental setup. We used 32 DFB-LDs as signal light sources, which were equally spaced by 0.5nm in the wavelength range 1543.2–1558.7nm. Each odd and even channel was combined separately in an array waveguide grating (AWG) and then through two $LiNbO_3$ Mach-Zehnder external modulators for data coding and amplitude modulation. In addition, slight phase modulation was applied to improve the transmission performance. The pulsewidth was ~40ps. After producing two sets of pre-chirped 10.66Gbit/s, 2^{23}–1 return to zero (RZ) signals, they were combined using a polarisation beam splitter and launched into the transmission line in the orthogonal state of polarisation with each other [4]. The 280km circulating loop consisted of six 47km long spans of transmission fibre and seven 980nm pumped erbium doped fibre amplifier repeaters (EDFAs). We used two kinds of fibres to configure all the fibre spans. The first segment following after the EDFAs was standard SMF and the second segment SCDCF, which has a negative dispersion and negative dispersion slope to form dispersion flattened transmission spans. The typical parameters of each fibre are listed in Table 1. To compensate for the residual dispersion and dispersion slope of the loop, SCDCF with a dispersion of –400ps/nm/km was inserted at the beginning of the loop. The average dispersion slope of the circulating loop was only 0.005ps/nm^2/km and the average dispersion at 1550 nm was 0.27 ps/nm/km. The loss of transmission spans including splicing loss was 11.3dB on average. The 980nm pumped single-stage EDFAs had